

# Adaptive Space-Time Decision Feedback Neural Detectors with Data Selection for High-Data Rate Users in DS-CDMA Systems

Rodrigo C. de Lamare and Raimundo Sampaio-Neto

**Abstract**—A space-time adaptive decision feedback (DF) receiver using recurrent neural networks (RNN) is proposed for joint equalization and interference suppression in direct-sequence code-division-multiple-access (DS-CDMA) systems equipped with antenna arrays. The proposed receiver structure employs dynamically driven RNNs in the feedforward section for equalization and multi-access interference suppression and a finite impulse response (FIR) linear filter in the feedback section for performing interference cancellation. A data selective gradient algorithm, based upon the set-membership design framework, is proposed for the estimation of the coefficients of RNN structures and is applied to the estimation of the parameters of the proposed neural receiver structure. Simulation results show that the proposed techniques achieve significant performance gains over existing schemes.

**Index Terms**—DS-CDMA, multiuser detection, neural networks, space-time processing, adaptive receivers, set-membership techniques.

## I. INTRODUCTION

CODE division multiple access (CDMA) implemented with direct sequence (DS) spread-spectrum signalling is currently deployed in many wireless communication systems. Such services include third-generation (3G) cellular telephony, indoor wireless networks, terrestrial and satellite communication systems. The advantages of CDMA include good performance in multi-path channels, flexibility in the allocation of channels, increased capacity in bursty and fading environments and the ability to share bandwidth with narrow-band communication systems without deterioration of either's systems performance [1], [2].

The capacity of a DS-CDMA network is limited by different types of interference, namely, narrowband interference (NBI), multi-access interference (MAI), inter-symbol interference (ISI) and the noise at the receiver. The major source of interference in most CDMA systems is MAI, which is highly structured and arises due to the fact that users communicate through the same physical channel with non-orthogonal signals. The multiple propagation paths of the channel can destroy the orthogonality of the signals at the receiver, giving rise to MAI even when the users employ orthogonal signatures. For non-orthogonal signatures the channel and the lack of

synchronism between users can further increase the level of MAI. The conventional (single-user) receiver that employs a filter matched to the signature sequence does not suppress MAI and is very sensitive to differences in power between the received signals (near-far problem). In order to mitigate the effect of interference in CDMA systems, a designer can resort to multiuser detection techniques for MAI suppression, and antenna arrays, which perform spatial filtering and can reduce the impact of interference. The optimal multiuser detector of Verdu [3] suffers from exponential complexity and requires the knowledge of timing, amplitude and signature sequences. This has motivated the development of various sub-optimal strategies: the linear [4] and decision feedback [5] receivers, the successive interference canceller [6] and the multistage detector [7]. The combination of multiuser detection and beamforming can provide an enhanced performance for MAI and ISI suppression [1], [2]. This requires the joint processing of the data received at an antenna array with elements closely spaced and the estimation of the direction of arrival (DoA) and the channel information.

In current third-generation (3G) wireless cellular communications, there are some specific features in the operation of the systems such as the use of antenna arrays by the base stations for increasing the capacity in the uplink (mobile terminals to base station) and different data rates and quality of service requirements [8]. In particular, third-generation wideband DS-CDMA systems have multi-code capabilities, in which the user signals with high data rate (HD) can be accommodated by reducing the processing gain  $N_h$  and using a low spreading factor and higher power levels [8]. In these scenarios, users are equipped with multiple processing gains, operate at different data rates, and HD users operate at higher signal-to-noise ratios (SNRs). The SNR is proportional to their data rates, which leads to a situation where they experience a relatively low level of MAI but more significant level of ISI. In contrast, low data rate (LD) users, that work with larger spreading factors and lower SNRs, encounter higher levels of MAI and near-far effects.

In order to design an effective space-time receiver for interference mitigation in DS-CDMA systems employing multi-code capabilities and antenna arrays, we investigate in this work the use of receiver structures based on recurrent neural networks and decision feedback schemes. One motivation for this work is that neural networks provide good nonlinear mapping of the inverse model of the channel and can deal with the uncertainty and interference present in the received data.

Dr. R. C. de Lamare is a Lecturer with the Communications Research Group, Department of Electronics, University of York, York YO10 5DD, United Kingdom and Prof. R. Sampaio-Neto is with CETUC/PUC-RIO, 22453-900, Rio de Janeiro, Brazil. E-mails: rcd1500@ohm.york.ac.uk, raimundo@cetuc.puc-rio.br

Therefore, receivers based on neural networks outperform those based on FIR linear filters. Despite the increased complexity over receivers with FIR linear filters, the deployment of neural structures is feasible in situations where the number of processing elements is not very large, i.e., the spreading factor of CDMA systems is low and the number of HD users is small. Such situations appear in the context of 3G wireless communications [8]. Recent work on equalization and modelling of nonlinear systems has shown that recurrent neural networks (RNNs) are superior in bit error rate (BER) performance to multilayer perceptrons (MLPs), radial basis functions (RBFs) [9] and FIR linear filters. Prior work on equalization structures also demonstrated that decision feedback (DF) neural equalization structures are better than neural schemes without DF and DF and linear equalizers with linear FIR filters [10]. In the context of CDMA systems, existing works on neural and related structures are restricted to MLPs [11], RBFs [12], support vector machines (SVMs) [13] and to static channels, and little attention has been given to RNNs and DF structures. This is especially relevant for the uplink of wireless communications systems, where the base station can afford an antenna array and more complex algorithms as compared to the mobile terminals. In this case, the trade-off between computational complexity and superior performance is quite attractive.

In order to estimate the parameters of the receiver, a designer must resort to a training algorithm. Amongst the available training methods for neural detectors, one can employ gradient based approaches such as the back propagation algorithm for MLPs [9] and the real time recurrent learning (RTRL) or fast least-squares (LS) and Kalman-based techniques [14] for RNNs. On one hand, gradient-type approaches for neural schemes are simpler to implement, exhibit low complexity but possess slow convergence rates and have to deal with the problem of vanishing gradients [9] for RNNs. On the other hand, LS and Kalman algorithms have fast convergence but exhibit very high computational complexity and numerical problems for implementation. This motivates the search for novel approaches to training RNNs that possess fast convergence, low complexity and flexibility. The algorithm can be also applied to problems such as estimation and tracking of non-linear and dynamic processes and modelling of time-varying non-linear systems [9]. In this context, set-membership (SM) filtering [15], [16] represents a class of recursive estimation algorithms that, on the basis of a pre-determined error bound, seeks a set of parameters that yield bounded output errors. In particular, the SM approach leads to low-complexity gradient algorithms with excellent convergence and tracking performance due to the use of an adaptive step size and data selective updates. The appealing feature of SM algorithms is that they are able to significantly improve the convergence and tracking of estimators and possess a complexity lower than conventional estimation algorithms due to their sparse updates. The existing works on SM algorithms deal with the adaptation of linear FIR filters and there is no SM algorithm for training important neural structures such as RNNs available.

In this work, our first contribution is to present an adaptive

space-time adaptive DF multiuser receiver structure for HD users with antenna arrays, using dynamically driven RNNs [9] in the feedforward section and FIR linear filters in the feedback section for cancelling the associated HD and LD users. These RNNs have not been considered for the problem of space-time multiuser detection so far. The advantage of antenna arrays lies in the spatial separation of the interfering users, increasing the capacity of the system. The proposed structure employs antenna arrays combined with a neural RNN processor and a DF structure, which are shown to provide considerable capacity gains over schemes with FIR linear filters. The second contribution of this work is the development of a novel data-selective algorithm for parameter estimation in RNNs using the set-membership estimation framework [15], [16]. The proposed algorithm is applied here to the problem of space-time neural receivers for DS-CDMA systems, even though, the algorithm is general and can be used for other applications of neural networks. It should also be remarked that some very recent contributions [17]-[24], which constitute the state-of-the-art in the area of RNN, can be considered for further investigation in the context of interference mitigation in communication systems such as CDMA, OFDM and MIMO [25]. However, we have opted to focus here on a RNN scheme combined with FIR filters in a decision feedback architecture, its application to space-time CDMA systems and the development of a novel estimation technique.

This paper is structured as follows. Section II briefly describes the space-time DS-CDMA communication system model and formulates the problem. The proposed space-time DF neural receivers for joint equalization and multiuser detection are presented in Section III. The novel set-membership adaptive algorithms for the neural structures are presented in Section IV. Section V is dedicated to the presentation and discussion of the simulation results and Section VI gives the concluding remarks of this work and comments on possible extensions and future work.

## II. SPACE-TIME DS-CDMA SYSTEM MODEL AND PROBLEM STATEMENT

Let us consider the uplink of an asynchronous multi-code QPSK DS-CDMA system with  $L$  paths and 2 classes of  $K = K_h + K_l$  users, where  $K_h$  is the number of HD users with  $N_h$  chips per symbol and  $K_l$  the number of LD users with  $N_l$  chips per symbol, as depicted in Fig. 1. These QPSK symbols are spread with unique sequences for each user, modulated and transmitted over a communication channel. At the receiver equipped with antenna arrays, the composite signal is demodulated, sampled at chip rate and applied to a bank of filters matched to the users' effective spatial spreading sequences. In what follows, we mathematically detail these operations and describe the signal processing.

The transmitted signal for the  $k$ th user amongst the HD

users and the  $q$ th user amongst the LD users are given by

$$\begin{aligned} x_k^h(t) &= A_k^h \sum_{i=-\infty}^{\infty} b_k^h(i) s_k^h(t - iT_h) \\ x_q^l(t) &= A_q^l \sum_{i=-\infty}^{\infty} b_q^l(i) s_q^l(t - iT_l) \end{aligned} \quad (1)$$

where the equiprobable symbols  $b_k^h(i)$  and  $b_q^l(i) \in \{\pm 1, \pm j\}/\sqrt{2}$  with  $j^2 = -1$  denote the  $i$ -th symbol for users  $k$  and  $q$ , the real valued spreading waveforms and the amplitude associated with HD user  $k$  and LD user  $q$  are  $s_k^h(t)$ ,  $s_q^l(t)$ ,  $A_k^h$  and  $A_q^l$ , respectively.

The spreading waveforms for the HD and LD users are expressed by  $s_k^h(t) = \sum_{i=1}^{N_h} a_k^h(i) \phi(t - iT_c)$  and  $s_q^l(t) = \sum_{i=1}^{N_l} a_q^l(i) \phi(t - iT_c)$ , respectively, where  $a_k^h(i) \in \{\pm 1/\sqrt{N_h}\}$ ,  $a_q^l(i) \in \{\pm 1/\sqrt{N_l}\}$ ,  $\phi(t)$  is the chip waveform,  $T_c$  is the chip duration and  $N_h = T_h/T_c$  and  $N_l = T_l/T_c$  are the processing gains of the HD and LD users, respectively. In practice, HD users can use  $N_h = \beta N_l$ , being  $\beta = 2, 4, 8, 16, 32$ , the smallest  $N_l = 8$  and the largest  $N_h = 256$  [31]. Assuming that the receiver with linear antenna arrays is synchronized with the main path and identical fading is experienced by all antenna elements for each path of each user signal, the coherently demodulated composite received signal at the  $p$ th antenna element is

$$\begin{aligned} r_p(t) &= \sum_{k=1}^{K_h} \sum_{m=0}^{L-1} h_{k,m}^h(t) e^{-j\Theta_{k,m}^h} x_k^h(t - \tau_{k,m}^h - d_k^h) \\ &+ \sum_{q=1}^{K_l} \sum_{m=0}^{L-1} h_{q,m}^l(t) e^{-j\Theta_{q,m}^l} x_q^l(t - \tau_{q,m}^l - d_q^l) + n(t) \end{aligned} \quad (2)$$

where  $\Theta_{k,m}^h = 2\pi(p-1)(d/\lambda) \sin(\phi_{k,m}^h)$  and  $\Theta_{q,m}^l = 2\pi(p-1)(d/\lambda) \sin(\phi_{q,m}^l)$  are the delay shifts of the  $m$ th path of the  $k$ th HD user and the  $q$ th LD user, respectively. The quantities  $\phi_{k,m}^h$  and  $\phi_{q,m}^l$  are the directions of arrival (DoA) of the signals of the HD user  $k$  and LD user  $q$  and their  $m$ th paths,  $d = \lambda/2$  is the spacing between sensors and  $\lambda$  is the carrier wavelength. The channel coefficients associated with the  $m$ -th path and the  $k$ -th HD user are  $h_{k,m}^h(t)$ ,  $d_k^h \in [0, N_h)$  is the delay of the  $k$ th user taken from a discrete uniform random variable between 0 and  $N_h$  and  $\tau_{k,m}^h$  is the delay of the  $m$ th path of the  $k$ th user, whereas the channel coefficients associated with the  $m$ -th path and the  $q$ -th LD user are  $h_{q,m}^l(t)$ ,  $d_q^l \in [0, N_l)$  is the delay of the  $q$ th user taken from a discrete uniform random variable between 0 and  $N_l$  and  $\tau_{q,m}^l$  is the delay of the  $m$ th path of the  $q$ th LD user. The coefficients of the channels for both LD and HD users are modelled as a tapped-delay-line and their coefficients can be computed according to an available standard such as the UMTS model [31].

We assume that the delays are multiples of the chip periods, the channel is constant during each symbol interval (the coherence time of the channel does not exceed that of the symbol - this is typical in 3G systems [8]), the spreading codes are repeated from symbol to symbol, and the receiver with a  $J$ -element linear antenna array is perfectly synchronized

with the main path. The complex envelope of the received waveforms after filtering by a chip-pulse matched filter and sampled at chip rate yields the discrete-time samples for the user of interest at the  $p$ th antenna element

$$\begin{aligned} r_p(n) &= \sum_{k=1}^{K_h} \sum_{m=0}^{L-1} h_{k,m}^h e^{-j\Theta_{k,m}^h} x_{k,m}^h(nT_c - \tau_{k,m}^h - d_k^h) \\ &+ \sum_{q=1}^{K_l} \sum_{m=0}^{L-1} h_{q,m}^l e^{-j\Theta_{q,m}^l} x_{q,m}^l(nT_c - \tau_{q,m}^l - d_q^l) + n_p(n) \end{aligned} \quad (3)$$

By collecting these samples from each antenna element and organizing them into a  $JM \times 1$  observation vector corresponding to the  $i$ th signalling interval, we obtain

$$\mathbf{r}(i) = \sum_{k=1}^{K_h} \mathbf{x}_k(i) + \sum_{q=1}^{K_l} \mathbf{z}_q(i) + \boldsymbol{\eta}(i) + \mathbf{n}(i) \quad (4)$$

where  $M = N_h + L - 1$ , the  $k$ th HD user signal is given by  $\mathbf{x}_k(i)$ , the  $q$ th asynchronous signal of LD users that impinges on the antenna array is represented by  $\mathbf{z}_q(i)$ . The  $(JM \times 1)$  vector  $\mathbf{z}_q(i)$  is given by  $\mathbf{z}_q(i) = [z_{q,1}(i) \dots z_{q,JM}(i)]^T$ , where  $z_{q,n}(i) = \sum_{m=0}^{L-1} h_{q,m}^l e^{-j\Theta_{q,m}^l} x_{q,m}^l(nT_c - \tau_{q,m}^l - d_q^l)$ .

The complex Gaussian noise vector is  $\mathbf{n}(i) = [n_1(i) \dots n_{JM}(i)]^T$  with zero mean and  $E[\mathbf{n}(i)\mathbf{n}^H(i)] = \sigma^2 \mathbf{I}$ ,  $(\cdot)^T$  and  $(\cdot)^H$  denote transpose and Hermitian transpose, respectively, the operator  $E[\cdot]$  stands for expected value, and  $\boldsymbol{\eta}(i)$  is the intersymbol interference (ISI) vector. Indeed, the  $JM \times 1$  vector of ISI  $\boldsymbol{\eta}(i)$  is constructed with linear combinations of the channel coefficients, the symbols from previous, current and succeeding symbols and chips of the spreading codes of the HD users, similarly to  $\mathbf{z}_q(i)$ . In this model, the ISI span and contribution  $\boldsymbol{\eta}[i]$  are functions of the processing gain  $N_h$  of HD users and the number of paths  $L$ . If  $1 < L \leq N_h$  then 3 symbols would interfere in total, the current one, the previous and the successive symbols. In the case of  $N_h < L \leq 2N_h$  then 5 symbols would interfere, the current one, the 2 previous and the 2 successive ones. In most practical CDMA systems, we have that  $1 < L \leq N_h$  and then only 3 symbols are usually affected. The reader is referred to [1] for further details related to the ISI and models. The UMTS channel models [31], which reveal that the channel usually affects at most 3 symbols (it typically spans a few chips) provides further details about the typical channels. In the case of HD users it is substantially more significant due to the ratio  $L/N_h$  which is greater than  $L/N_l$ .

The main problem is how to detect the HD users with the minimum probability of error possible and at reasonably complexity. The minimum probability of error detector was proposed by Verdu [2], [3] and corresponds to a combinatorial problem with exponential complexity with the number of users. In what follows, we seek the design of a high-performance detector with affordable complexity by proposing a decision feedback structure with recurrent neural networks.

### III. PROPOSED SPACE-TIME DECISION FEEDBACK NEURAL RECEIVER

The space-time decision feedback receiver structure, depicted in Fig. 2, applies a bank of ST-RAKE detectors [25] to the observation vector  $\mathbf{r}(i)$ , followed by a neural MUD that employs dynamically driven recurrent neural networks (RNNs) in the feedforward section for suppressing MAI and ISI and an FIR linear filter in the feedback section for cancelling the associated users in the system. The RNNs [9] used in the multiuser detector (MUD) are small structures, with feedback connections and where each artificial neuron is connected to the others, capable of achieving superior performance to MLPs and RBFs [9]. In this context, the advantage of the neural MUD over linear ones is the use of non-linear mappings to create decision boundaries for the detection of transmitted symbols.

We consider a one shot approach (detection of the symbols corresponding to one time instant) where the  $K_h \times 1$  input vector  $\mathbf{u}(i) = [u_1(i) \dots u_{K_h}(i)]^T$  to the MUD is given by

$$\mathbf{u}(i) = \mathbf{S}^H \mathbf{r}(i), \quad (5)$$

where  $\mathbf{S} = [\tilde{\mathbf{s}}_1^a \dots \tilde{\mathbf{s}}_{K_h}^a]$  and  $\tilde{\mathbf{s}}_k^a$  is the user  $k$  effective spatial signature of the  $k$ th HD user that assumes the knowledge (or estimates) of the DOAs and channels or their estimates. The spatial signature  $\tilde{\mathbf{s}}_k^a$  results from the convolution of the original signature sequence  $\mathbf{s}_k^h$  with the channel and the time shifts resulting from the antenna array, and can be represented as

$$\tilde{\mathbf{s}}_k^a = [\tilde{\mathbf{s}}_{k,1}^T \dots \tilde{\mathbf{s}}_{k,p}^T \dots \tilde{\mathbf{s}}_{k,J}^T]^T, \quad (6)$$

where  $\tilde{\mathbf{s}}_{k,p} = [\tilde{s}_{k,p,1} \dots \tilde{s}_{k,p,M}]^T$  is the  $M \times 1$  signature at the  $p$ th antenna of the receiver.

Let us now describe in detail the schematic of the proposed space-time decision feedback neural receiver depicted in Fig. 2. Specifically, the proposed receiver design is equivalent to processing the output  $\mathbf{u}(i)$  of the bank of ST-RAKE detectors with the RNN in the feedforward part of the receiver and the decision feedback section. The  $K_h \times 1$  data vector  $\mathbf{u}(i)$  is stacked with the  $Q \times 1$  vector of states of the RNN

$$\mathbf{x}_k(i-1) = \varphi(\mathbf{W}_k^H(i)\boldsymbol{\xi}_k(i)), \quad (7)$$

where the matrix  $\mathbf{W}_k(i) = [\mathbf{w}_{k,1}(i) \dots \mathbf{w}_{k,j}(i) \dots \mathbf{w}_{k,Q}(i)]$  with dimensions  $(Q+K_h) \times Q$  and whose  $Q$  columns  $\mathbf{w}_{k,j}(i)$ , with  $j = 1, 2, \dots, Q$  have dimensions  $(Q+K_h) \times 1$  contain the coefficients of the RNN receiver for user  $k$  and  $\varphi(\cdot)$  is the activation function of the RNN and which is used to form the  $(Q+K_h) \times 1$  vector

$$\boldsymbol{\xi}_k(i) = [\mathbf{x}_k^T(i-1) \mathbf{u}^T(i)]^T, \quad (8)$$

which is processed by the neural part of the receiver. The activation function is chosen as  $\varphi(\cdot) = \tanh(\cdot)$  in order to limit the amplitude range of the output signals of the network and to avoid numerical instability in the recurrent structure [?]. In particular, the  $\tanh(\cdot)$  fits well in communications problems as it provides naturally a soft estimate of symbols. In the case of DS-CDMA systems, it provides a soft estimate which is fed back to the neural structure and helps it to inversely map

the symbol estimate appropriately in the presence of multiple-access interference and noise. The RNN in the feedforward section then processes  $\boldsymbol{\xi}_k(i)$  to yield the initial decisions as given by

$$\begin{aligned} \hat{b}_k(i) &= v(\mathbf{D}\mathbf{x}_k(i)) = \text{sgn}(\Re[\mathbf{D}\mathbf{x}_k(i)]) + \text{jsgn}(\Im[\mathbf{D}\mathbf{x}_k(i)]) \\ &= \text{sgn}(\Re[\mathbf{D}\varphi(\mathbf{W}_k^H(i)\boldsymbol{\xi}_k(i))]) + \text{jsgn}(\Im[\mathbf{D}\varphi(\mathbf{W}_k^H(i)\boldsymbol{\xi}_k(i))]), \end{aligned} \quad (9)$$

where  $v(\cdot)$  denotes a slicing function that contains the operators  $\Re(\cdot)$  and  $\Im(\cdot)$  which are used to select the real and imaginary parts, respectively, and then quantizes the output of each operator in order to detect the QPSK symbols. The matrix  $\mathbf{D} = [1 \ 0 \ \dots \ 0]$  is the  $1 \times Q$  matrix that defines the number of outputs of the network and  $\text{sgn}(\cdot)$  is the signum function. Since we are only interested in one symbol at each time instant the vector  $\mathbf{D}$  has this structure which means that only one output of the RNN is used to yield the symbol estimate. The initial symbol estimates for each user (including the HD users and the LD users which use an MMSE linear receiver [2]) are then stacked in order to form the  $K \times 1$  vector with the initial decisions  $\hat{\mathbf{b}}(i) = [\hat{b}_1(i) \ \hat{b}_2(i) \ \dots \ \hat{b}_K(i)]$ . The estimate of the desired symbol for user  $k$  at symbol  $i$  then becomes:

$$z_k(i) = \mathbf{D}\varphi(\mathbf{W}_k^H(i)\boldsymbol{\xi}_k(i)) - \mathbf{f}_k^H(i)\hat{\mathbf{b}}(i), \quad k = 1, 2, \dots, K_h \quad (10)$$

where the  $K \times 1$  vector  $\mathbf{f}_k$  ( $k = 1, 2, \dots, K_h$ ) represents the feedback filters used to cancel the interference contribution of the associated users. In particular, the feedback filter  $\mathbf{f}_k(i)$  of user  $k$  has a number of non-zero coefficients corresponding to the available number of feedback connections for each type of cancellation structure. The final detected QPSK symbol is:

$$\begin{aligned} \hat{b}_k^f(i) &= \text{sgn}(\Re[z_k(i)]) + \text{jsgn}(\Im[z_k(i)]) \\ &= \text{sgn}(\Re[\mathbf{D}\varphi(\mathbf{W}_k^H(i)\boldsymbol{\xi}_k(i)) - \mathbf{f}_k^H(i)\hat{\mathbf{b}}(i)]) + \text{jsgn}(\Im[\mathbf{D}\varphi(\mathbf{W}_k^H(i)\boldsymbol{\xi}_k(i)) - \mathbf{f}_k^H(i)\hat{\mathbf{b}}(i)]), \end{aligned} \quad (11)$$

Regarding the structure of the decision feedback (DF) section, the literature reports two basic types of feedback, namely, the successive DF [7] and the parallel DF [27]. For successive DF (S-DF) [26] and a system with an equal number of feedback entries and users  $K$ , we have the  $K \times K$  matrix  $\mathbf{F}(i) = [\mathbf{f}_1(i) \ \dots \ \mathbf{f}_{K_h}(i)]$ , which is formed with the filters for the  $K$  users, is strictly lower triangular, whereas for parallel DF (P-DF) [27]  $\mathbf{F}(i)$  is full and constrained to have zeros on the main diagonal in order to avoid cancelling the desired symbols. The S-DF structure is optimal in the sense of that it achieves the sum capacity of the synchronous CDMA channel with AWGN [26]. In addition, the S-DF scheme is less affected by error propagation although it generally does not provide uniform performance over the user population, which is a desirable characteristic for uplink scenarios. In this context, the P-DF system can offer uniform performance over the users but it suffers from error propagation in low signal-to-noise ratios (SNRs) and high bit error rates (BERs). In order to design the DF receivers and satisfy the constraints of the associated structures, the designer must obtain the vector with initial

decisions  $\bar{\mathbf{b}}(i)$  and then perform to the adopted cancellation approach.

Unlike prior work, we focus on a scenario where there are  $K_h$  HD users, i.e.,  $K_h$  feedback filters  $\mathbf{f}_k(i)$  with dimensions  $K \times 1$  as the filters are also supposed to cancel the contribution of the LD users. Thus, in this case the matrix of cancellation filters  $\mathbf{F}(i) = [\mathbf{f}_1(i) \ \mathbf{f}_2(i) \ \dots \ \mathbf{f}_{K_h}(i)]^T$  has dimensions  $K \times K_h$ . Due to its property of offering uniform performance over the user population and better performance as compared to S-DF schemes [27], [28], [29], we will adopt P-DF schemes and introduce a modification for including the LD users in the cancellation process. The feedback connections used and their associated number of non-zero filter coefficients in  $\mathbf{f}_k$  are equal to  $K - 1$  for the HD users. The resulting matrix  $\mathbf{F}(i)$  for the proposed neural receiver is full and constrained to have zeros on the diagonal from the first row to the  $K_h$ th row in order to avoid cancelling only the desired symbols of the HD users. The rest of the matrix is full such that all LD are addressed by the feedback section.

#### IV. SET-MEMBERSHIP ADAPTIVE ALGORITHMS

Set-membership filtering (SMF) [15], [16] represents a class of recursive estimation algorithms that, on the basis of a pre-determined error bound, seeks a set of parameters that yield bounded filter output errors. These algorithms have been used in a variety of applications such as adaptive equalization [16] and multi-access interference suppression [16]. The SMF algorithms are able to combat conflicting requirements of fast convergence and low misadjustment by introducing a modification on the objective function. In addition, these algorithms exhibit reduced complexity due to data-selective updates, which involve two steps: a) information evaluation and b) update of parameter estimates. If the filter update does not occur frequently and the information evaluation does not involve much computational complexity, the overall complexity can be significantly reduced. The adaptive SMF algorithms usually achieve good convergence and tracking performance due to an adaptive step size for each update, and reduced complexity resulting from data selective updating.

In this section, a novel efficient parameter estimator for neural structures based on the SMF framework [15], [16] is described. Unlike prior work on FIR filters, we propose set-membership (SM) algorithms for RNNs structures. In the SM framework, the receiver weight vectors  $\mathbf{w}_{k,j}(i)$  and  $\mathbf{f}_k(i)$  are designed to achieve a specified bound on the magnitude of the estimation error  $e_k(i) = b_k(i) - (\mathbf{D}\mathbf{x}_k(i) - \mathbf{f}_k^H(i)\hat{\mathbf{b}}(i))$ . As a result of this constraint, the SM adaptive algorithm will only perform filter updates for certain data. Let  $\Theta_k(i)$  represent the set containing all  $\mathbf{w}_{k,j}(i)$  and  $\mathbf{f}_k(i)$  that yield an estimation error upper bounded in magnitude by  $\gamma$ . Thus, we can write

$$\Theta_k(i) = \bigcap_{(\mathbf{u}(i), b_k(i)) \in \mathbf{S}} \{ \mathbf{w}_{k,j}, \in \mathcal{C}^{(Q+K_h)}, \mathbf{f}_k \in \mathcal{C}^K : |e_k(i)| \leq \gamma \} \quad (12)$$

where  $\mathbf{S}$  is the set of all possible data pairs  $(\mathbf{u}(i), b_k(i))$  and the set  $\Theta_k(i)$  is referred to as the feasibility set and any point in it is a valid estimate  $z_k(i)$ . Since it is not practical to predict all data pairs, adaptive methods work with the membership

sets  $\psi_{k,i} = \bigcap_{m=1}^i \mathcal{H}_{k,m}$  provided by the observations, where  $\mathcal{H}_{k,m} = \{ \mathbf{w}_{k,j}, \in \mathcal{C}^{(Q+K_h)}, \mathbf{f}_k \in \mathcal{C}^K : |b_k(m) - z_k(m)| \leq \gamma \}$ . In order to derive an SM adaptive algorithm using point estimates for the proposed DF receiver structure, we consider the cost function

$$\mathcal{L}(\mathbf{W}_k(i), \mathbf{f}_k(i)) = E[|b_k(i) - (\mathbf{D}\mathbf{x}_k(i) - \mathbf{f}_k^H(i)\hat{\mathbf{b}}(i))|^2] \quad (13)$$

subject to  $|e_k(i)| \leq \gamma$ , where  $e_k(i) = b_k(i) - (\mathbf{D}\mathbf{x}_k(i) - \mathbf{f}_k^H(i)\hat{\mathbf{b}}(i))$ . A gradient algorithm can be developed by computing the gradient terms with respect to  $\mathbf{w}_{k,j}$  and  $\mathbf{f}_k$ , and using their instantaneous values. Firstly, we consider the first partial derivative of  $\mathcal{L}(\mathbf{W}_k(i), \mathbf{f}_k(i))$  with respect to the parameter vector  $\mathbf{w}_{k,j}(i)$  with dimension  $(Q + K_h) \times 1$ , which forms the matrix  $\mathbf{W}_k$

$$\begin{aligned} \frac{\partial \mathcal{L}(\mathbf{W}_k(i), \mathbf{f}_k(i))}{\partial \mathbf{w}_{k,j}^*(i)} &= \left( \frac{\partial e_k(i)}{\partial \mathbf{w}_{k,j}^*(i)} \right) e_k^*(i) = -\mathbf{D} \left( \frac{\partial \mathbf{x}_k(i)}{\partial \mathbf{w}_{k,j}^*(i)} \right) e_k^*(i) \\ &= -\mathbf{D}\mathbf{\Lambda}_{k,j}(i)e_k^*(i) \end{aligned} \quad (14)$$

where the  $K_h \times (Q + K_h)$  matrix  $\mathbf{\Lambda}_{k,j}(i)$  contains the partial derivatives of the state vector  $\mathbf{x}_k(i)$  with respect to  $\mathbf{w}_{k,j}(i)$ . To obtain the expressions for updating the matrix  $\mathbf{\Lambda}_{k,j}(i)$ , we consider the update equations for the state vector  $\mathbf{x}_k(i)$  given through (7) and (8). Using the chain rule of calculus in (8), we obtain a recursion that describes the dynamics of the learning process of the neural section of the receiver:

$$\mathbf{\Lambda}_{k,j}(i+1) = \mathbf{\Phi}_k(i) \left( \mathbf{W}_k^{1:K}(i)\mathbf{\Lambda}_{k,j}(i) + \mathbf{U}_{k,j}(i) \right), \quad j = 1, \dots, K \quad (15)$$

where the  $Q \times Q$  matrix  $\mathbf{W}_k^{1:K}$  denotes the submatrix of  $\mathbf{W}_k$  formed by the first  $K_h$  rows of  $\mathbf{W}_k$ , the  $Q \times Q$  matrix  $\mathbf{\Phi}_k(i)$  for user  $k$  has a diagonal structure where the elements correspond to the partial derivative of the activation function  $\varphi(\cdot)$  with respect to the argument  $\mathbf{w}_{k,j}^H(i)\boldsymbol{\xi}_k(i)$  as given by

$$\mathbf{\Phi}_k(i) = \text{diag} \left( \varphi'(\mathbf{w}_{k,1}^H(i)\boldsymbol{\xi}_k(i)), \dots, \varphi'(\mathbf{w}_{k,K}^H(i)\boldsymbol{\xi}_k(i)) \right) \quad (16)$$

where the  $K_h \times (Q + K_h)$  matrix  $\mathbf{U}_{k,j}(i) = [\mathbf{0}^T \ \boldsymbol{\xi}_k^T(i) \ \mathbf{0}^T]^T$  has all the rows with zero elements, except for the  $j$ -th row that is equal to the vector  $\boldsymbol{\xi}_k(i)$ . By using a gradient optimization that uses the rules  $\mathbf{w}_{k,j}(i+1) = \mathbf{w}_{k,j}(i) - \mu_n \frac{\partial \mathcal{L}(\mathbf{W}_k(i), \mathbf{f}_k(i))}{\partial \mathbf{w}_{k,j}^*(i)}$ ,  $\mathbf{f}_k(i+1) = \mathbf{f}_k(i) - \mu_f \frac{\partial \mathcal{L}(\mathbf{W}_k(i), \mathbf{f}_k(i))}{\partial \mathbf{f}_k^*(i)}$  and substituting (14) and  $\frac{\partial \mathcal{L}(\mathbf{W}_k(i), \mathbf{f}_k(i))}{\partial \mathbf{f}_k^*(i)} = e_k^*(i)\hat{\mathbf{b}}(i)$ , we obtain

$$\mathbf{w}_{k,j}(i+1) = \mathbf{w}_{k,j}(i) + \mu_n \mathbf{D}\mathbf{\Lambda}_{k,j}(i)e_k^*(i) \quad (17)$$

$$\mathbf{f}_k(i+1) = \mathbf{f}_k(i) - \mu_f \hat{\mathbf{b}}(i) \quad (18)$$

In order to ensure the constraint on the error bound ( $|e_k(i)| \leq \gamma$ ), we substitute (17) into (13) and then we make the terms equal to  $\gamma$ . We proceed with the feedback filter  $\mathbf{f}_k(i)$  in the same way, which yields the algorithms

$$\mathbf{w}_{k,j}(i+1) = \begin{cases} \mathbf{w}_{k,j}(i) + \frac{(1 - \frac{\gamma}{|e_k(i)|})}{\|\mathbf{\Lambda}_{k,j}(i)\|^2} \mathbf{D}\mathbf{\Lambda}_{k,j}(i)e_k^*(i) & \text{if } |e_k(i)| > \gamma \\ \mathbf{w}_{k,j}(i) & \text{otherwise} \end{cases} \quad (19)$$

$$\mathbf{f}_k(i+1) = \begin{cases} \mathbf{f}_k(i) - \frac{(1 - \frac{\gamma}{|e_k(i)|})}{(\hat{\mathbf{b}}^H(i)\mathbf{b}(i))} e_k^*(i) \hat{\mathbf{b}}(i) & \text{if } |e_k(i)| > \gamma \\ \mathbf{f}_k(i) & \text{otherwise} \end{cases} \quad (20)$$

where  $\mu_n = (1 - \frac{\gamma}{|e_k(i)|}) / \|\mathbf{A}_{k,j}(i)\|^2$  and  $\mu_f = (1 - \frac{\gamma}{|e_k(i)|}) / (\hat{\mathbf{b}}^H(i)\mathbf{b}(i))$  are the new normalized step sizes of the algorithms. The novel adaptive technique is called the SM normalized real time recurrent learning (SM-NRTRL) algorithm. It introduces a powerful variable step size and discerning update rule.

## V. SIMULATION EXPERIMENTS

In this section we assess the performance of the proposed space-time neural receivers and SM algorithms in terms of the bit error rate (BER). We compare the proposed neural MUD (NMUD) and DF neural MUD (DF-NMUD) receivers with the RAKE [25], the linear MUD (L-MUD) and the DF-MUD with  $J = 1$  and their space-time versions with  $J = 2, 3$  antenna elements. We also evaluate the convergence performance of the adaptive estimation algorithms, i.e., the NLMS, the NRTRL [9], the SM-NLMS [15] and the proposed SM-NRTRL. For the NMUD we make  $\mathbf{f}_k = \mathbf{0}$  in the structure and algorithms of Sections III and IV.

The DS-CDMA system employs, QPSK modulation, Gold sequences of length  $N = 7$  or random sequences of length  $N = 8$  for the HD users and Gold sequences of length  $N_l = 31$  for the LD users and the number of HD and LD users is equal ( $K_l = K_h$ ) in all experiments. We adopted an identical ratio of LD to HD users for simplicity. In a practical system, it is expected that the number of LD users significantly exceed the HD ones since the LD users correspond to voice users (major part of users and market), whereas the HD users correspond to multimedia and data users. Another issue is that since a number of DS-CDMA systems in use include higher-order modulation schemes, besides QPSK, it should be noted that the proposed system can be modified to handle higher-order modulation schemes such as QAM-16 and QAM-64. In this case, it would be necessary to modify the detection rule in the receiver. Specifically, the slicer would have to take into account the different levels of the signal constellation. The LD users also operate asynchronously with single-antenna MMSE linear receivers [25] and a power level 3 dB below that of HD users. The channels experienced by different users are i.i.d. whose coefficients for each user  $k$  ( $k = 1, \dots, K$ ) are  $h_{k,l}(i) = p_l \alpha_{k,l}(i)$ , where  $p_l$  are the gains (or average powers) of the channel paths (power delay profile) and  $\alpha_{k,l}(i)$  ( $l = 0, 1, \dots, L-1$ ) are complex Gaussian random sequences obtained by passing complex white Gaussian noise through a filter with approximate transfer function  $c/\sqrt{1 - (f/f_d)^2}$  where  $c$  is a normalization constant,  $f_d = v/\lambda$  is the maximum Doppler shift,  $\lambda$  is the wavelength of the carrier frequency, and  $v$  is the speed of the mobile [30]. The channel powers are normalized so that  $\sum_{l=1}^{L_p} p_l^2 = 1$ . This procedure corresponds to the generation of independent sequences of correlated unit power Rayleigh random variables ( $E[|\alpha_{k,l}^2(i)|] = 1$ ). We show the results in terms of the normalized Doppler frequency  $f_d T$  (cycles/symbol) and use three-path channels with relative average powers  $p_l$  given by 0, -3 and -6 dB, where in each

run the spacing between paths is obtained from a discrete uniform random variable (d.u.r.v.) between 1 and 3 chips.

The asynchronism  $\tau_k$  in chips is taken from a d.u.r.v between 1 and the respective processing gain of the class of user (HD or LD). The parameters of the algorithms are optimized and the system has perfect power control between users of each class (HD or LD). The activation function  $\varphi(\cdot)$  for the neural receivers is the hyperbolic tangent, the number of states  $Q$  of the RNNs is set to 1, the DOAs  $\phi_{k,m}$  are uniformly distributed in  $(-\pi/3, \pi/3)$  for all simulations and the NLMS is used to estimate the effective spatial signature of the receiver structure. Experiments are averaged over 200 independent runs and the parameter  $\gamma$  was chosen as  $\sqrt{3.5\sigma^2}$  for the neural MUDs and  $\sqrt{5\sigma^2}$  for the other detectors. The proposed and existing algorithms are all initialized with parameter vectors with zero elements in order to provide a fair comparison. The BER performance shown in the results refers to the average BER amongst the  $K_h$  HD users.

In Figs. 3 and 4 we show the BER convergence performance of the analyzed algorithms and linear and DF receivers, respectively. We also include the Kalman algorithm of [14] with  $J = 3$  and the proposed neural structure in the comparison as an upper bound. The curves show that data-selective algorithms outperform the conventional adaptive techniques both in convergence speed and steady-state performance, while they only perform filter updates for a fraction of the overall symbols. The DF schemes, shown in Fig. 4, and in particular the DF-NMUD outperform the schemes without DF, shown in Fig. 3, and as the number of antenna elements  $J$  is increased so is the performance. The proposed SM-NRTRL algorithm for the neural structure outperforms the NRTRL and has a performance very close to the Kalman technique of [14], which has much higher complexity ( $O(K_h^3)$ ).

In terms of complexity, the algorithms require  $O(QK_h)$  for training the neural structures and  $O(K)$  for training the linear filters but the SM-NRTRL neural algorithms exhibit better performance and lower UR. Indeed, the update rate (UR) of the SM algorithms is shown in Table I at  $E_b/N_0 = 10\text{dB}$  and  $f_d T = 0.0001$ , where it is shown the advantage in terms of UR of the neural approach combined with SM framework. The UR depends on  $f_d T$  and  $\gamma$ , and we verified that, for an extensive set of scenarios, the SM-NRTRL has the ability to consistently operate at lower UR than existing algorithms. The complexity is mainly dictated by the number of states  $Q$  of the neural network and the number of HD users  $K_h$ . The number of antenna elements  $J$  increases the complexity of the space-time receivers in an identical way for both neural and non-neural schemes because the in the proposed structure the signal processing either via neural structures or linear ones is performed after the bank of ST-RAKE receivers. In this case, we used NLMS algorithms to estimate the effective spatial signatures of the users, which despread the signals prior to the processing of the receiver.

The BER performance of SM-adaptive algorithms and DF receivers is shown in Fig. 5. The receivers are adjusted with 200 symbols during the training period, then switch to decision-directed mode and process 2000 data symbols. The results show that the proposed DF-NMUD achieves the best

BER performance, followed by the DF-MUD with linear filters (DF-MUD), and the RAKE receivers.

In the last experiment, shown in Fig. 6, we consider randomly generated sequences with  $N = 8$  and receivers with single antennas and space-time receivers with  $J = 3$  antenna elements in order to evaluate a situation that may arise in a practical standard, i.e., the 3G UMTS system. In this case, the channels are modeled by the UMTS Vehicular A channel model [31] with maximum Doppler frequency  $f_D = 100$  Hz with a carrier frequency  $f_c = 2$  GHz. The receivers are adjusted with 200 symbols during the training period, then switch to decision-directed mode and process 2000 data symbols. The curves show that the proposed DF-NMUD achieves the best BER performance, followed by the remaining techniques, corroborating the results obtained for the previous experiments.

## VI. CONCLUSIONS AND FUTURE WORK

A space-time adaptive DF neural receiver for high rate users in DS-CDMA systems was proposed for joint equalization and multiuser detection. In order to estimate the parameters of the proposed receiver, we developed a low complexity data-selective algorithm was developed based on the concept of Set-Membership filtering. Numerical results have shown that the proposed neural structure and algorithms considerably outperform existing methods. For future work, the proposed scheme and algorithms can also be considered and applied to other communications systems such as MIMO systems. Detectors with attractive trade-off between performance and complexity such as the proposed one are of central importance in MIMO systems. This would require a description of a discrete-time model of MIMO systems and a formulation of the problem involving the application of the proposed DF neural structure for extracting the desired signals embedded in interference. Future work may also involve the investigation of novel adaptive estimation algorithms using the set-membership framework. Algorithms with faster convergence rate than the one proposed here such as least squares and those with data reuse may be of interest for the estimation of parameters in a larger neural structure, as well as, the formulation of set-membership techniques with automatic adjustment of the bound.

## REFERENCES

- [1] M. L. Honig and H. V. Poor, "Adaptive interference suppression," in *Wireless Communications: Signal Processing Perspectives*, H. V. Poor and G. W. Wornell, Eds. Englewood Cliffs, NJ: Prentice-Hall, 1998, ch. 2, pp. 64-128.
- [2] S. Verdú, *Multiuser Detection*, Cambridge University Press, New York: 1998.
- [3] S. Verdú, "Minimum Probability of Error for Asynchronous Gaussian Multiple-Access Channels," *IEEE Trans. Info. Theory*, vol.IT-32, no. 1, pp. 85-96, January 1986.
- [4] R. Lupas and S. Verdú, "Linear multiuser detectors for synchronous code-division multiple-access channels," *IEEE Trans. Inform. Theory*, vol. 35, pp. 123-136, 1989.
- [5] M. Abdulrahman, A. U.K. Sheikh and D. D. Falconer, "Decision Feedback Equalization for CDMA in Indoor Wireless Communications," *IEEE Journal on Selected Areas in Communications*, vol 12, no. 4, pp. 698 - 706, May 1994.
- [6] P. Patel and J. Holtzman, "Analysis of a Simple Successive Interference Cancellation Scheme in a DS/CDMA Systems", *IEEE Journal on Selected Areas in Communications*, vol. 12, n. 5, pp. 796 - 807, June 1994.
- [7] M. K. Varanasi and B. Aazhang, "Multistage detection in asynchronous CDMA communications," *IEEE Transactions on Communications*, vol. 38, no. 4, pp. 509-19, April, 1990.
- [8] "Physical Layer Standard for CDMA2000 Spread Spectrum Systems (Release C)," Telecommunications Industry Association, TIA/EIA/IS-2002.2-C, May 2002.
- [9] S. Haykin, *Neural Networks: A Comprehensive Foundation*, 2nd Edition, Prentice-Hall, 1999.
- [10] S. Ong, C. You, S. Choi and D. Hong, "A decision feedback recurrent neural equalizer as an infinite impulse response filter," *IEEE Transactions on Signal Processing*, vol. 45, no. 11, pp. 2851 - 2858, November 1997.
- [11] B. Aazhang, B. P. Paris and G. C. Orsak, "Neural Networks for Multiuser Detection in Code-Division-Multiple-Access Communications," *IEEE Transactions on Communications*, vol. 40, No. 7, pp. 1212 - 1222, July 1992.
- [12] U. Mitra and H. V. Poor, "Neural Network Techniques for Adaptive Multi-user Demodulation," *IEEE Journal on Selected Areas of Communications*, Vol. 12, No. 9, pp. 1460 - 1470, December 1994.
- [13] S. Chen, A. K. Samigan, and L. Hanzo, "Support vector machine multiuser receiver for DS-CDMA signals in multipath channels," *IEEE Trans. on Neural Networks*, vol. 12, pp. 604-611, 2001.
- [14] J. Choi, A. C. C. de Lima, S. Haykin, "Kalman Filter-Trained Recurrent Neural Equalizers for Time-Varying Channels," *IEEE Transactions on Communications*, vol. 53, no. 3, pp. 472 - 480, March 2005.
- [15] S. Gollamudi, S. Nagaraj, S. Kapoor and Y. F. Huang, "Set-Membership Filtering and a Set-Membership Normalized LMS Algorithm with an Adaptive Step Size," *IEEE Signal Processing Letters*, vol. 5, No. 5, pp. 111 - 114, May 1998.
- [16] S. Gollamudi, S. Kapoor, S. Nagaraj and Y. F. Huang, "Set-Membership Adaptive Equalization and an Updater-Shared Implementation for Multiple Channel Communication Systems", *IEEE Trans. on Sig. Proc.*, vol. 46, no. 9, pp. 2372-2385, September 1998.
- [17] Y. Xia and J. Wang, "A recurrent neural network for solving nonlinear convex programs subject to linear constraints", *IEEE Transactions on Neural Networks*, vol. 16, no. 2, March 2005, pp. 379 - 386.
- [18] J. Choi, M. Bouchard and T. H. Yeap, "Decision feedback recurrent neural equalization with fast convergence rate", *IEEE Transactions on Neural Networks*, vol. 16, no. 3, May 2005 pp. 699 - 708.
- [19] Y. Zhang and S. S. Ge, "Design and analysis of a general recurrent neural network model for time-varying matrix inversion", *IEEE Transactions on Neural Networks*, vol. 16, no. 6, Nov. 2005, pp. 1477 - 1490.
- [20] J.-S. Wang and Y.-P. Chen, "A fully automated recurrent neural network for unknown dynamic system identification and control", *IEEE Transactions on Circuits and Systems I: Regular Papers*, vol. 53, no. 6, June 2006, pp. 1363 - 1372.
- [21] A. Savran, "Multifeedback-Layer Neural Network", *IEEE Transactions on Neural Networks*, vol. 18, no. 2, March 2007, pp. 373 - 384.
- [22] Y. Xia and M. S. Kamel, "Cooperative Recurrent Neural Networks for the Constrained  $L_1$  Estimator", *IEEE Transactions on Signal Processing*, vol. 55, no. 7, Part 1, July 2007, pp. 3192 - 3206.
- [23] Y. Wu, Q. Song and S. Liu, "A Normalized Adaptive Training of Recurrent Neural Networks With Augmented Error Gradient", *IEEE Transactions on Neural Networks*, vol. 19, no. 2, Feb. 2008, pp. 351 - 356.
- [24] M. Delgado, M. P. Cuellar, and M. C. Pegalajar, "Multiobjective Hybrid Optimization and Training of Recurrent Neural Networks", *IEEE Transactions on Systems, Man, and Cybernetics, Part B*, vol. 38, no. 2, April 2008, pp. 381 - 403.
- [25] A. Paulraj, R. Nabar, D. Gore, *Introduction to Space-Time Wireless Communications*, Cambridge University Press, New York, 2003.
- [26] M. K. Varanasi and T. Guess, "Optimum decision feedback multiuser equalization with successive decoding achieves the total capacity of the Gaussian multiple-access channel," in *Proc. 31st Asilomar Conf. Signals, Systems and Computers*, Monterey, November 1997, pp. 1405-1409.
- [27] G. Woodward, R. Ratasuk, M. L. Honig e P. Rapajic, "Minimum Mean-Squared Error Multiuser Decision-Feedback Detectors for DS-CDMA," *IEEE Transactions on Communications*, vol. 50, no. 12, pp. 2104-2112, December, 2002.

- [28] R.C. de Lamare, R. Sampaio-Neto, "Adaptive MBER decision feedback multiuser receivers in frequency selective fading channels", *IEEE Communications Letters*, vol. 7, no. 2, Feb. 2003, pp. 73 - 75.
- [29] R.C. de Lamare, R. Sampaio-Neto, "Minimum Mean-Squared Error Iterative Successive Parallel Arbitrated Decision Feedback Detectors for DS-CDMA Systems", *IEEE Transactions on Communications*, vol. 56, no. 5, May 2008, pp. 778 - 789.
- [30] T. S. Rappaport, *Wireless Communications*, Prentice-Hall, Englewood Cliffs, NJ, 1996.
- [31] Third Generation Partnership Project (3GPP), specifications 25.101, 25.211-25.215, versions 5.x.x.

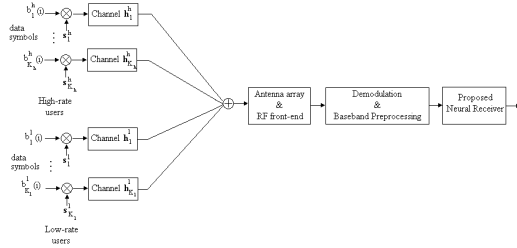


Fig. 1.

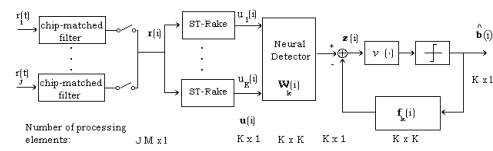


Fig. 2.

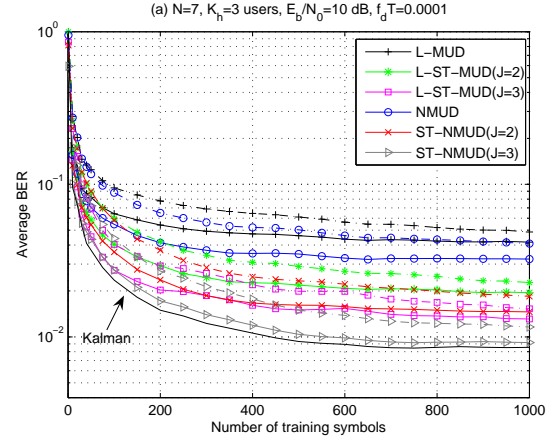


Fig. 3.

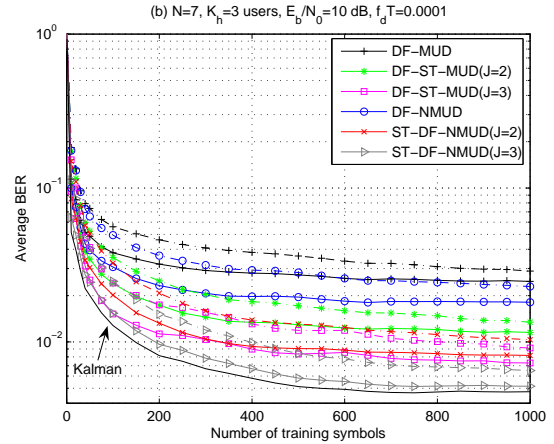


Fig. 4.

### Captions:

Fig. 1: Block diagram of the space-time DS-CDMA system model.

Fig. 2: Block diagram of the proposed space-time decision feedback neural receiver.

Fig. 3: BER convergence performance of data-selective and conventional (dash-dotted lines) algorithms for linear receivers.

Fig. 4: BER convergence performance of data-selective and conventional (dash-dotted lines) algorithms for DF receivers.

Table 1: Update Rate of SM algorithms at  $E_b/N_0 = 10dB$  and  $f_d T = 0.0001$ .



TABLE I

Detectors	L-MUD	NMUD	DF-MUD	DF-NMUD
J=1	25.4%	18.2%	24.6%	15.7%
J=2	24.5%	17.1%	23.1%	14.3%
J=3	23.9%	16.8%	21.5%	13.8%

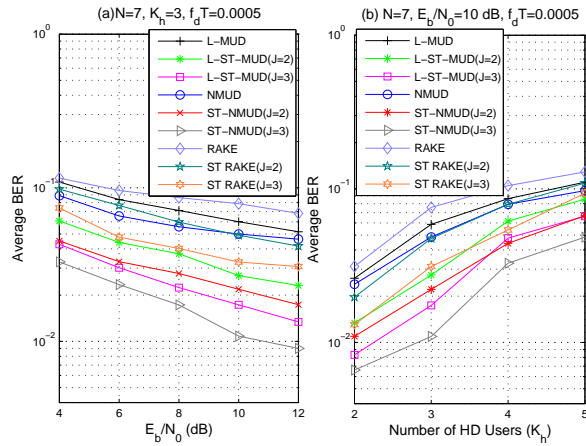


Fig. 5.

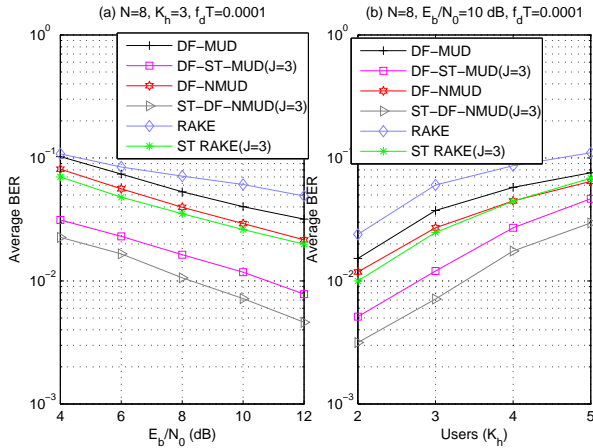


Fig. 6.

Fig. 5: BER performance of DF receivers versus (a)  $E_b/N_0$  and (b) number of HD users ( $K_h$ ).

Fig. 6: BER performance of DF receivers versus (a)  $E_b/N_0$  and (b) number of HD users ( $K_h$ ) for a UMTS channel model.